

## The effect of replacing steel reinforcements with GFRP on the torsional behavior of RC L-shaped beams

Amin Saleh<sup>1</sup>, M. Hamed<sup>2</sup>, A. Deifalla<sup>3</sup> and T. Ali<sup>4</sup>

<sup>1</sup> Professor, Ain Shames University, Cairo, Egypt

<sup>2</sup> Graduate Student, Ain Shames University, Cairo, Egypt

<sup>3</sup> Lecturer, British University Egypt, El-Shourouk, Egypt

<sup>4</sup> Professor, Helwan University, Cairo, Egypt

**ABSTRACT:** The failure of structural elements caused by corrosion of conventional steel reinforcements directed researchers all over the world to investigate the repairing of existing steel RC elements or find viable substitutes for reinforcing new RC elements. For existing structural elements, FRP fabrics are being studied as external reinforcement for the purpose of repairing RC elements deteriorated due to corrosion of steel reinforcements. On the other hand, for new structural elements, FRP bars are being investigated as non-corrosive internal reinforcements. The torsional behavior of FRP-internally reinforced concrete beams was not fully investigated. Previous studies showed that bended GFRP stirrup is inadequate. In this paper, a new technique for forming the stirrup without bent is introduced. In addition, the effectiveness of replacing steel bars and/or steel stirrups with GFRP bars and/or glued GFRP stirrups for reinforcing L-shaped beams under torsion is examined. Three L-shaped beams were constructed and tested using a test setup that subjects L-shaped beams to pure torsion. The three beams has the same cross section dimensions and reinforcement ratios, however, the first beam has steel longitudinal and transversal reinforcements, the second beam has GFRP longitudinal reinforcements and steel transversal reinforcements, and the third beam has GFRP longitudinal and transversal reinforcements. It was found that using glued GFRP as transversal reinforcements improve the ultimate strength, cause slightly wider cracks and large deformations up till the ultimate load. In addition, The PCI (2006) was used to estimate the ultimate strength. It was found to be in good agreement with the experimental results, however, conservative by more than 11%.

### 1 INTRODUCTION

The long-term durability of RC concrete structures has become a major concern in the construction industry. The corrosion of steel reinforcement reduces the durability and the service life of RC structures. Many steel-reinforced concrete structures are exposed to deicing salts and marine environments which eventually require extensive and expensive maintenance. For over a decade, fiber reinforced polymer (FRP) fabrics are being studied as external reinforcement in order to repair RC beams under torsion (Deifalla et. al. 2013). On the other hand, to have highly durable concrete structures with long service life, the usage of FRP as an alternative reinforcing material is a feasible solution. In addition to the noncorrosive nature of FRP materials, they have a high strength-to-weight ratio that makes them attractive as internal reinforcements for concrete structures. The first design guide for FRP-internally reinforced

concrete elements was published in Japan (JSCE, 1997). Since then, the usage of FRP materials as reinforcement for concrete elements is rapidly increasing. Today, FRP reinforcing bars are produced by a number of companies in North America, Asia, and Europe. The usage of FRP bars has become main stream and is no longer confined to research projects. Extensive research programs have been conducted to investigate the flexural behavior of FRP internally reinforced concrete beams (El-Salakawy and Benmokrane 2004). On the other hand, very few studies were directed towards the shear behavior of FRP internally reinforced concrete beams. Due to urgent need, although research is still ongoing on this area, several new releasers of the codes and design guidelines addressing FRP bars as internal longitudinal reinforcement for structural concrete is still being published (ACI 2006). However, the validity of these design provisions is still being investigated. El-Sayed et. al. (2006) examined the design provisions for calculating the concrete contribution to the shear strength of beams with only longitudinal FRP bars and without stirrups. In this study, two parameters were investigated; the reinforcement ratio and the modulus of elasticity of the FRP bars. In addition, very limited number of studies investigated the shear design of RC beams with FRP stirrups; however, it has not yet been fully explored. Last but not least, the torsion behavior of FRP internally reinforced beams with or without stirrups is a new area. A study by Shehab et. al. (2009) showed that the FRP stirrup bended using gentle heating exhibit a strength reduction which might lead to inadequate performance under torsion. The objective of this research is to investigate the torsion behavior of concrete beams reinforced longitudinally and transversely with GFRP bars. Three L-shaped beams were constructed and tested using a test setup that is capable of subjecting L-shaped beams to pure torsion. The three beams had the same longitudinal and transversal reinforcement ratios. The main parameter investigated was using GFRP bars versus conventional steel bars as longitudinal and/or transversal reinforcement. The experimental results were reported and analyzed. Figure (1) shows an internal reinforcement cage with the glued GFRP stirrups. The behavior of the L-shaped beams in terms of cracking strength, ultimate strength and corresponding deformations. An analytical estimation is presented which was found in good agreement with the experimental results.



Figure 1: FRP cage

## 2 EXPERIMENTAL PROGRAM

### 2.1 *Material properties*

Three materials were used in the experimental program; Concrete, Steel and GFRP. Each material was tested separately to determine its mechanical properties. Slump test result was 75 mm. Concrete compressive strength after 27 days was 25 MPa. Two types of steel were used; mild steel for transversal reinforcement with nominal yield strength value of 240 MPa and High grade steel for longitudinal reinforcement with a nominal yield strength value of 360 MPa. Both steel types had a young's modulus of 210 GPa. The GFRP had a stress – strain behavior as shown in figure 2. The behavior is linear up till failure with a fracture strength value of 400 MPa and young's modulus of 36.7 GPa.

### 2.2 *Specimen details*

Three beams were tested under torsion. The three beams had the same L-shaped cross section dimensions. The total height, flange width, web width and flange thickness were 350, 300, 150 and 150 mm, respectively. The longitudinal and transversal reinforcements were as shown in Table 1.

Table 1. Specimen reinforcement's details

Specimen	Longitudinal	Transversal
LB1	2Ø12 T&B (High grade steel)	7Ø6/m' (mild steel)
LB2	2Ø12 T&B (GFRP)	7Ø6/m' (mild steel)
LB3	2Ø12 T&B (GFRP)	7Ø6/m' (GFRP)

### 2.3 *Test setup and instrumentations*

Figure 3 shows a schematic diagram for the test setup. All tested beams had a total length 1.60 m. Beams were vertically supported at a distance 1.45 m center to center. These supports ensured that the beam was free to twist and elongate longitudinally during the test. The load was applied through a diagonally placed steel spreader beam on the ends of two steel arms with length 0.4 m. These arms were fixed at the end parts of each tested beam as shown in Figure 3. Details of the typical dimensions, typical reinforcements, dial gauge locations and strain gauge locations for all beams are shown in Figure 4. The concrete cover is 25 and 15 mm for the web and the flange, respectively. The load was imposed at a single point in the middle of the spreader beam which was measured by a load cell. Electrical strain gauges were used to measure strain in the steel stirrups and the longitudinal steel reinforcement as shown in figure 4. Deflection was calculated as the average of the measured value of the two dial gauges assembled at the edges of the test zone.

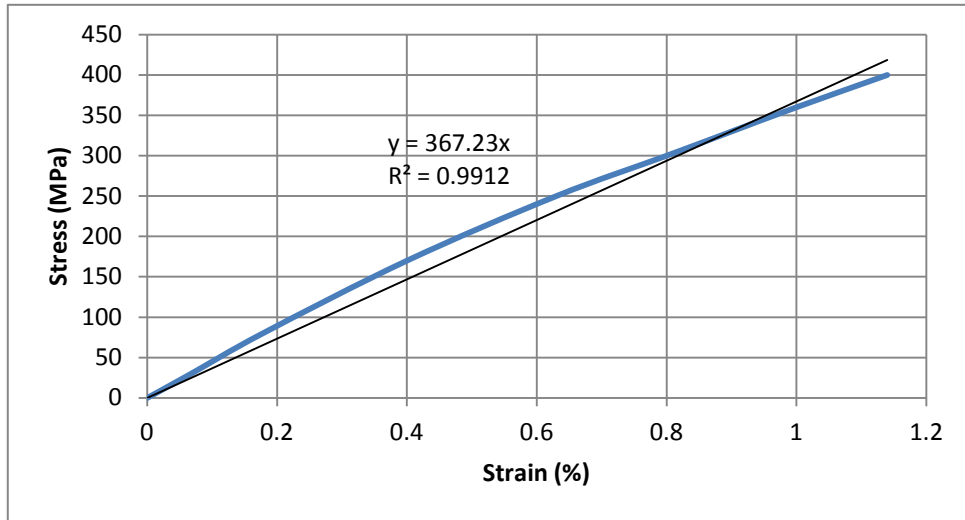


Figure 2: Typical Stress-strain behavior of GFRP coupons

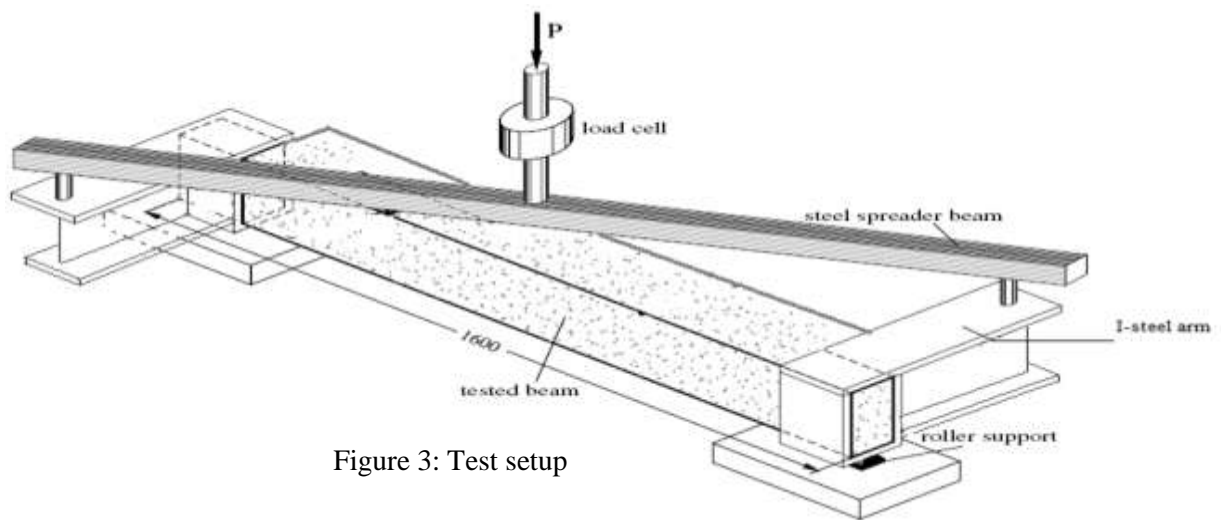


Figure 3: Test setup

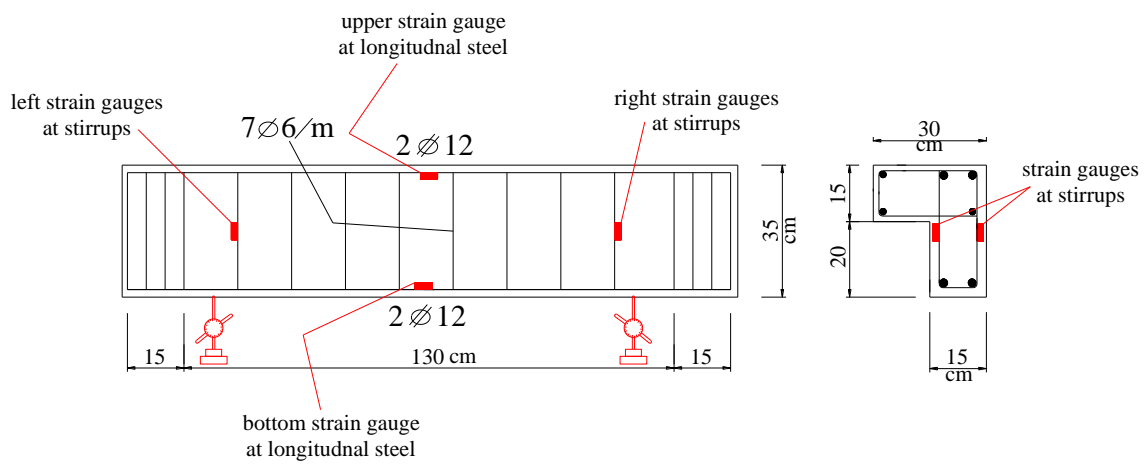


Figure 4: Strain gauge location

#### 2.4 Specimen preparation

The three L-shaped beams were poured together and cast in a clean wooden forms stiffened with vertical supports every 300 mm to maintain the L-shape. The forms were laid leveled on the concrete floor. The beams were poured with the web vertical. The forms were painted on the inside with lubricating oil, which facilitates the removal of the forms after the concrete hardens. A slump test was carried out before concrete pouring to measure the workability of the concrete batch. During casting, 12 standard cylinders of 150 mm diameter and 300 mm height were poured. The cylinders were taken from the concrete batch when the beams were poured. The flange and the web of the beam were poured monolithically to ensure compatibility between them. The concrete was compacted using two electrical internal poker type vibrators. The concrete was moist cured using wet burlap for 7 days under controlled laboratory conditions. After that, the burlap and the wooden forms were removed and the beams were stored inside the laboratory until tested. Three cylinders were tested in compression after 7 days, three after 28 days and three on the day of the beams testing. Three split cylinder tests were done after 28 days.

#### 2.5 Test procedure

The same procedure was followed during the testing of the L-shaped beams to insure that all the tests were consistent. After installing the beam in the test setup and attaching the instruments, the beam was loaded with a small load within the elastic range of concrete to avoid cracks. The measurements from this initial testing were verified to ensure that all the instruments are correctly installed and functioning properly. All beams were tested to failure using the test setup. The load was applied to the beams manually using control pumps. In order to capture the full behavior, the loads were applied in small steps of 5 kN.

### 3 TEST RESULTS AND DISCUSSIONS

#### 3.1 LBI

The first observed crack was initiated at the middle of the web across the edge section at a load value of 10 kN. As the load increased, the initial crack propagated in an inclined spiral form around the perimeter of the beam cross section. New spiral cracks were initiated which were similar to the initial crack as for the propagation direction and inclination to the longitudinal axis of the beam. After concrete cracking, the strain in the transverse and longitudinal steel increased significantly. With further increase in the load, the cracks widened reaching the middle section of the beam. Spalling occurred in the flange at a load value of 30 kN, when small pieces of concrete started falling from the top of the flange. At a load value of 40 kN a major spiral crack close to the west end of the test region was formed. The test was terminated when the beam resistance dropped significantly. The beam failed after a major spiral crack was formed within the test zone. The beam achieved maximum load resistance of 41 kN. At the ultimate strength, the unit angle of twist, the vertical displacement, the stirrup strain, and the longitudinal strain were 3.06 deg/m<sup>2</sup>, 4.2 mm, 0.2 %, and 0.114 %, respectively.

### 3.2 *LB2*

The first observed crack was initiated at the middle of the web across the edge section at a load value of 10 kN. As the load increased, the initial crack propagated in an inclined spiral form around the perimeter of the beam cross section. New spiral cracks were initiated which were similar to the initial crack as for the propagation direction and inclination to the longitudinal axis of the beam. After concrete cracking, the strain in the transverse steel and longitudinal FRP increased significantly. With further increase in the load, the cracks widened reaching the middle section of the beam. Spalling occurred in the flange at a load value of 35 kN, when small pieces of concrete started falling from the top of the flange. At a load value of 40 kN a major spiral crack close to the west end of the test region was formed. The test was terminated when the beam resistance was about to dropped significantly. The beam achieved maximum load resistance of 42 kN. At the ultimate strength, the unit angle of twist, the displacement, the stirrup strain, and the longitudinal strain were 3.35 deg/m<sup>-1</sup>, 4.2 mm, 0.2 %, and 0.2 %, respectively.

### 3.3 *LB3*

The first observed crack was initiated at the middle of web across the edge section at a load value of 10 kN. As the load increased, the initial crack propagated towards the web in an inclined spiral form around the perimeter of the beam cross section. New spiral cracks were initiated which were similar to the initial crack as for the propagation direction and inclination to the longitudinal axis of the beam. After concrete cracking, the strain in the transverse and longitudinal steel increased significantly. With further increase in the load, the cracks widened reaching the middle section of the beam. Spalling occurred in the flange at a load value of 30 kN, when small pieces of concrete started falling from the top of the flange. At a load value of 45 kN a major spiral crack close to the west end of the test region was formed. The test was terminated when the beam resistance dropped significantly. The beam achieved maximum load resistance of 50 kN. At the ultimate strength, the displacement, stirrup strain, and longitudinal strain were 3.47 deg/m<sup>-1</sup>, 4.2 mm, 0.74 %, and 0.26 %, respectively.

### 3.4 *Load behavior*

Figure (5.a) shows the total applied load versus the vertical displacement for the tested beams. Figure (5.b) shows the total applied load versus the unit angle of twist for all the tested beams. The behavior was similar for all tested beams. All beams behaved linearly up till cracking and then went through a nonlinear stage up till failure. By comparing LB1 and LB2, we can conclude that the angle of twist for beam LB2 is 9% more than beam LB1. By comparing LB3 with LB2 and LB1, we can conclude that the angle of twist by beam LB3 is 13% more than LB1. In addition, the ultimate load for beam LB3 is 19% more than both LB1 and LB2.

### 3.5 *Cracking behavior*

Figure 7 shows the diagonal cracking pattern for beam LB3. All tested beams failed due to diagonal crushing of concrete in a brittle manner. However the steel reinforced beams did not exhibit many wide cracks or large deformations similar to the FRP reinforced beams at the maximum strength.

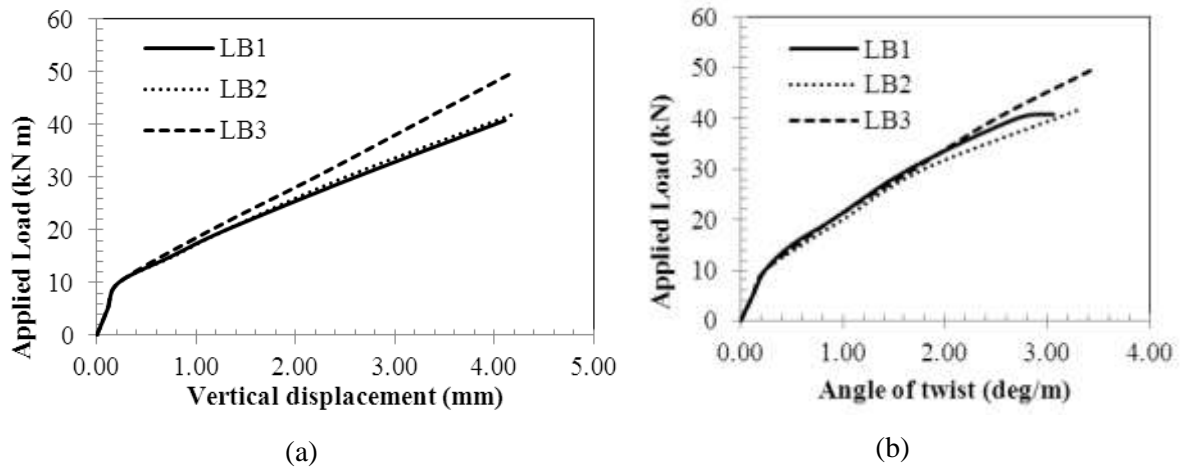


Figure 5: Load Behavior versus a) displacement and b) angle of twist.

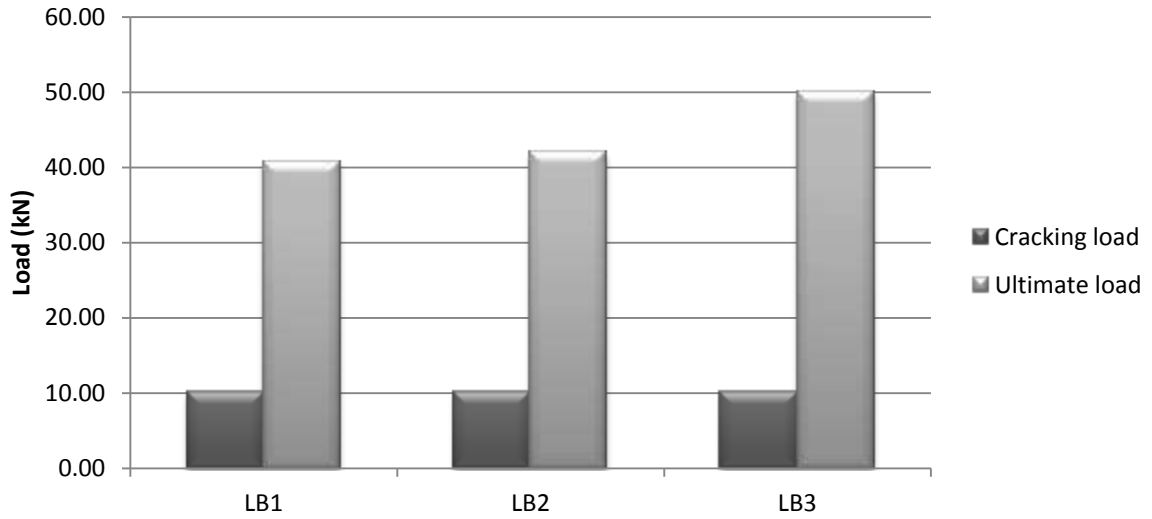


Figure 6: Cracking and Ultimate load



Figure 7: Failure mode of beam LB3

### 3.6 Analytical Estimation

Deifalla and Ghobarah (2005) assessed different design codes in regard of RC flanged beams and concluded that the PCI sixth edition (2006) provides better estimates for the ultimate strength. Consequently the PCI (2006) was adapted to calculate the ultimate torque capacity of the beams such that:

$$T = 0.0675\sqrt{f'_c} \sum x^2y + \frac{A_t}{s} \alpha_t x_1 y_1 f \dots \dots \dots \text{in SI units}$$

$f'_c$  is the compressive strength which was taken 25 MPa.  $x$  is the short side which was taken 150 mm for both the web and the flange.  $y$  is the long side which was taken 350 mm for the web and 150 mm for the flange.  $x_1$  is the short side of the closed tie which was taken 100 mm for both flange and web stirrup.  $y_1$  is the long side of the closed tie which was taken 300 for the web tie and 250 for the flange tie.  $A_t$  is the cross section area of one leg of the closed tie,  $s$  is the spacing between closed ties.  $\alpha_t = \left(0.66 + 0.33 \frac{y_1}{x_1}\right) < 1.5$  and  $f$  is the stress in the ties which was taken based on the experimentally recorded strain and Young's modulus values as shown in Table 2.

Table 2. Analytical Estimation

Specimen	Young's modulus (GPa)	Stirrup strain (%)	Calculated Torque (kN. m)	Experimental Torque (kN. m)	Error%
LB1	210	0.2	7.32	8.2	11
LB2	210	0.2	7.32	8.4	13
LB3	36.7	0.74	7.84	10	18

From the table it is clear that the PCI predictions for the ultimate torsion capacity of the RC beam with steel stirrups was accurate with 13% error. However, for the beam with GFRP stirrups, the error reached 18%. Moreover, it was found that conventional design codes are conservative. It can be concluded that further experimental studies is required to produce more accurate methods of estimating the ultimate capacity in the case of L-shaped beams with GFRP stirrups. Parameters that need to be investigated is the prediction of FRP strain and the angle of inclination used in the design. It is worth noting that the PCI is based on the skew bending theory with a 45 degree angle inclination which was is not necessary the case.

#### 4 FUTURE STUDIES

- Investigate the size effect of the cross section for beams with FRP stirrups under torsion.
- Explore the effect of the stirrups bars size for beams with FRP stirrups under torsion.
- Study the effect of the angle of inclination of the diagonal cracks and the effective strain in the stirrups on the behavior and design of beams with FRP stirrups under torsion.
- Develop numerical nonlinear models to predict the behavior of FRP internally reinforced beams under torsion and combined torsion.
- Propose design and analytical models for beams with FRP stirrups under torsion.

#### 5 CONCLUSIONS

The experimental results are limited, however, considered pilot in the field and the following can be concluded:

- The glued GFRP stirrup without bent can be used effectively as transversal reinforcement replacing conventional steel stirrup.
- Replacing the conventional steel stirrups with the glued GFRP stirrup increased the ultimate strength and corresponding displacement by 19.1% and 21.4%, respectively. They showed slightly wider cracks and large deformations at the same load over the steel transversally reinforced beams.
- The ultimate torsion capacity estimated by the PCI for the L-shaped RC beam was close, however, conservative by at least 11%.

#### ACKNOWLEDGMENT

The authors would like to express gratitude for the Civil Eng. Dept., Helwan University-Matria Branch for allowing the usage of their lab facility.

#### REFERENCES

- ACI 2006. Guide for the Design and Construction of Structural Concrete Reinforced with FRP Bars. ACI 440.1R-06, American Concrete Institute, Farmington Hills, MI.
- Deifalla, A., Awad, A., Abdelrahman, A. 2013. Load Capacity and Failure Modes of L-beams Strengthening Using FRP While Subjected to Pure Torsion. CSCE 2013, General Conference – Montreal, Quebec, May 29- June 1, GEN 153, 10 pp.
- Deifalla, A., Ghobarah, A. 2006. Experimentally Assessing the North American Design Codes Provisions for T-beams Under Torsion and Shear. Proceeding of the 7th International Conference on Short & Medium Span Bridges, Montreal, August 23-25, 2006, Paper No. 717.
- El-Salakawy, E., and Benmokrane, B., 2004. "Serviceability of Concrete Bridge Deck Slabs Reinforced with Fiber-Reinforced Polymer Composite Bars," ACI Structural Journal, 101(5), pp. 727-736.
- El-Sayed, A. K., El-Salakawy, E. F. and Benmokrane, B. 2006. Shear Strength of FRP-Reinforced Concrete Beams without Transverse Reinforcement. 103 (2), pp. 253-248.
- JSCE 1997. Recommendation for Design and Construction of Concrete Structures Using Continuous Fiber Reinforcing Materials. Concrete Engineering Series 23, Japan Society of Civil Engineers, Tokyo.
- PCI 2006, PCI design handbook precast and prestressed concrete. Chicago, Illinois 60606, pp. 736.
- Shهاب, H. K., H. S., El-Awady, M., Husain, M., and Mandour, S., 2009. Behavior of Concrete Beams Reinforced by FRP bars under Torsion. Proceedings of the 13<sup>th</sup> ICSGE, Cairo, Egypt, 12 pp.